



Article

Experimental Investigation on Flow Behavior of Paste Slurry Transported by Gravity in Vertical Pipes

Jiandong Wang ^{1,2,3} , Aixiang Wu ^{1,3}, Mi Wang ⁴ and Zhuen Ruan ^{1,2,3,*} 

¹ Key Laboratory of Ministry of Education for Efficient Mining and Safety of Metal Mines, University of Science and Technology Beijing, Beijing 100083, China

² Shunde Innovation School, University of Science and Technology Beijing, Foshan 528399, China

³ School of Civil and Resource Engineering, University of Science and Technology Beijing, Beijing 100083, China

⁴ School of Chemical and Process Engineering, University of Leeds, Leeds, West Yorkshire LS2 9JT, UK

* Correspondence: ustb_ruanzhuen@hotmail.com

Abstract: In order to dispose of large quantities of mineral tailings, paste backfill is proposed and widely adopted. Paste backfill, which has high concentration and yield stress and behaves as a non-Newtonian fluid, is prepared at the surface plant and then transported underground. Vertical pipelines are more likely to suffer various failures, such as pipe breaks, wear and plugging, during the transport process. Few present studies focus on the flow behavior of paste slurry flowing in vertical pipes. In this work, two L-shaped pipeline systems with internal diameters (ID) of 40 mm and 65 mm with electrical resistance tomography (ERT) were manufactured to visualize flow regimes and measure the axial velocity and pipe pressure of slurry flowing in the upper and lower zones of vertical pipes. Flow regimes were extracted from ERT-reconstructed images stacked by time-series. Based on this, four typical flow regimes were summarized, and the characteristics of velocity and pressure change with vertical pipe depth were discussed.

Keywords: paste slurry; vertical pipe; flow regime; axial velocity; pressure



Citation: Wang, J.; Wu, A.; Wang, M.; Ruan, Z. Experimental Investigation on Flow Behavior of Paste Slurry Transported by Gravity in Vertical Pipes. *Processes* **2022**, *10*, 1696. <https://doi.org/10.3390/pr10091696>

Academic Editor: Václav Uruba

Received: 3 August 2022

Accepted: 24 August 2022

Published: 26 August 2022

Publisher's Note: MDPI stays neutral with regard to jurisdictional claims in published maps and institutional affiliations.



Copyright: © 2022 by the authors. Licensee MDPI, Basel, Switzerland. This article is an open access article distributed under the terms and conditions of the Creative Commons Attribution (CC BY) license (<https://creativecommons.org/licenses/by/4.0/>).

1. Introduction

In recent decades, paste backfill technology has been extensively and increasingly used in mining operations to dispose of large quantities of mineral tailings [1], provide underground mine support and maximize ore recovery [2–5]. Paste backfill with a solids content of approximately 70 to 85 wt% [6,7], in which full tailings are bonded together by a hydraulic binder and mixing water [8], is prepared at the surface plant and then transported underground by gravity or a pumping system. It is clear that the most cost-effective transportation system is gravity. A common practice is to pour backfill into vertical pipes or boreholes which connect to horizontal pipes leading to the stope to be filled [9].

With the exhaustion of shallow resources, more and more mines with a depth of more than 1000 m have been built [10]. In the case of deep mines using the paste backfill method, gravity transport systems are preferred where possible and backfill will be conveyed over long distances which may include extra-long vertical pipes or boreholes. In this instance, vertical pipes or boreholes could easily suffer from pipeline vibration, blockage, water hammer and other failures as a result of the unsteady accelerated pipe flow, leading to high wear [11,12], fatigue damage or even bursting, which ultimately upsets the entire mining operation. Several photographs of vertical pipeline failures occurring in a metal mine in China using paste backfill are shown in Figure 1. Figure 1a presents one side of the pipe wall wearing faster than the other side. Figure 1b,c taken using a borehole endo-camera shows some scratches or even gaps in the inner pipe wall. Vertical delivery systems, generally buried between the ground surface and underground stopes, can be described as a black box where the internal backfill flow is not available for inspection. Avoiding backfill system failures and achieving high system reliability require a thorough understanding of

the flow behavior of paste backfill in vertical pipes. It is, therefore, necessary to examine how backfill slurry flows change with vertical pipe depth and to monitor flow parameters by adopting some investigative tools.

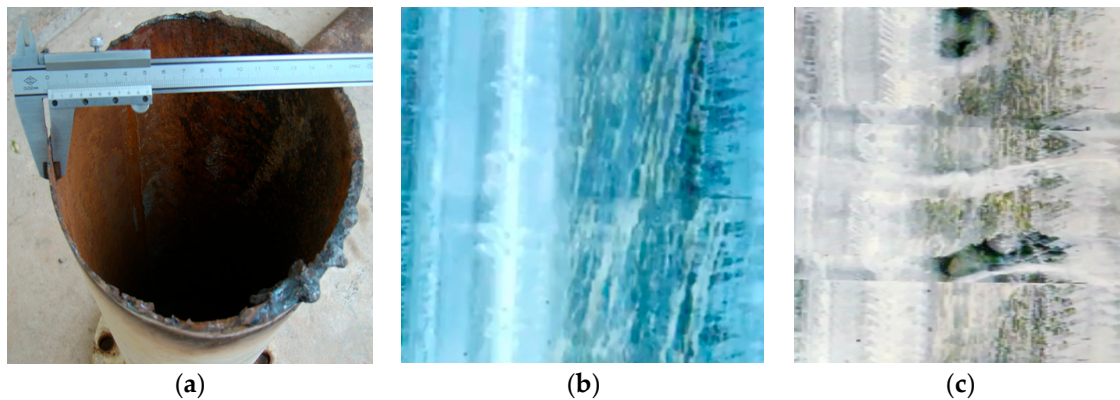


Figure 1. Several vertical pipeline failures (a) uneven wear (b) scratch and (c) gap.

Currently, a range of techniques, including optical methods [13,14], X-ray or gamma-ray scanning [15,16] and nuclear magnetic resonance imaging (MRI) [17,18] are applied to measure fluid flows. However, each of these techniques has its advantages and inherent limitations. For example, optical measuring methods can be quite difficult when testing opaque slurry flow. Some non-optical methods, such as X-ray and MRI, are very expensive and, more importantly, may cause environmental issues [19].

In the past decades, as a promising non-intrusive measurement technique, electrical resistance tomography (ERT) has received more attention from both academia and industry due to its advantages of fluid opacity independence, relatively low cost, no radiation hazard and online measurement [20,21]. ERT measurements has been widely used in mixing, transport and a few other processes [22–24]. For pipeline transport, ERT can obtain qualitative tomograms reflecting flow regimes and quantitative data that include cross-sectional profiles of the distribution of materials or velocities in pipes [25,26]. Applications of ERT to gas-liquid two-phase flow in the petrochemical field are more common in published literature [27–29]. ERT is also used to measure solid-liquid two-phase flow; however, most experimental studies take the slurry with concentrations of about 5–35% solid by volume as research objects [30–32]. Few researchers have successfully applied ERT measurements to paste slurry with very high solid content which is generally regarded as a non-Newtonian pseudo-plastic fluid [33].

Numerous researchers have performed extensive investigations on slurry pipeline transport. Horizontal pipe cases are greater in number compared to all other pipe configurations. Mechanisms describing the concentration distribution [20,34], flow properties [35–37] and pressure drop [38–40] across the flow have been understood to a certain extent. Nevertheless, very limited research has been performed on paste slurry flowing using gravity in vertical pipes. Existing related studies are generally based on ideal hypotheses or practical cases and lack visualization experiments using real-time monitoring system [41–43]. This is mainly due to the complexity of slurry gravity flow phenomena which makes it difficult to understand the flow.

This paper intends to evaluate the flow behavior of paste slurry transported by gravity flow. Two L-shaped pipeline systems with ERT were designed and manufactured to visualize flow regimes and measure the axial velocity and pipe pressure of paste slurry in vertical pipes. Several typical flow regimes were summarized, and the characteristics of axial velocity and pressure of slurry flowing in vertical pipes were discussed.

2. Experimental Setup and Methodology

2.1. Materials

Mineral tailings used in this experiment are from a Lead and Zinc Mine in Inner Mongolia, China. The specific gravity of the tailings measured using the water pycnometer test was 2.755 g/cm^3 . Particle size distribution was analyzed using a TopSizer Laser Particle Size Analyzer Instrument (OMEC Instruments Co., Ltd., Zhuhai, China), and the result is shown in Figure 2. The characteristic particle diameter D_x that represents the particle size with x vt% of tailings smaller than this size can be obtained from Figure 2. D_{10} , D_{50} and D_{90} of the tailings are 5.38, 56.60, 241.66 μm , respectively.

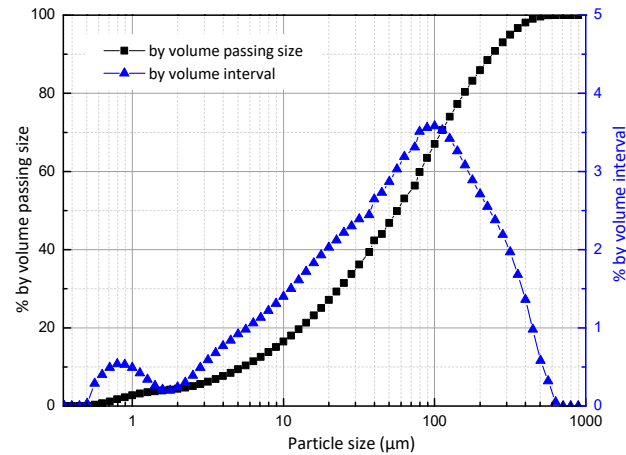


Figure 2. Particle size distribution of tailings.

Paste backfill generally contains mineral tailings, binder and water. However, cemented slurry solidification might do harm to ERT electrodes. The paste slurry prepared in this experiment consists only of the tailings and water and the binder was not included.

In order to determine slurry concentrations to be tested in the L-shaped pipeline systems, rheological parameters of slurries with different concentrations were tested using a Brookfield R/S plus rotor rheometer. Flow curves of these slurries are illustrated in Figure 3. The Bingham model was used to fit the flow curve. Bingham plastic viscosity and yield stress are listed in Table 1. Four slurry concentrations of 76%, 78%, 80% and 82% with yield stress of 7.16 Pa, 15.49 Pa, 35.25 Pa, 79.96 Pa, respectively, were used to carry out transport experiments.

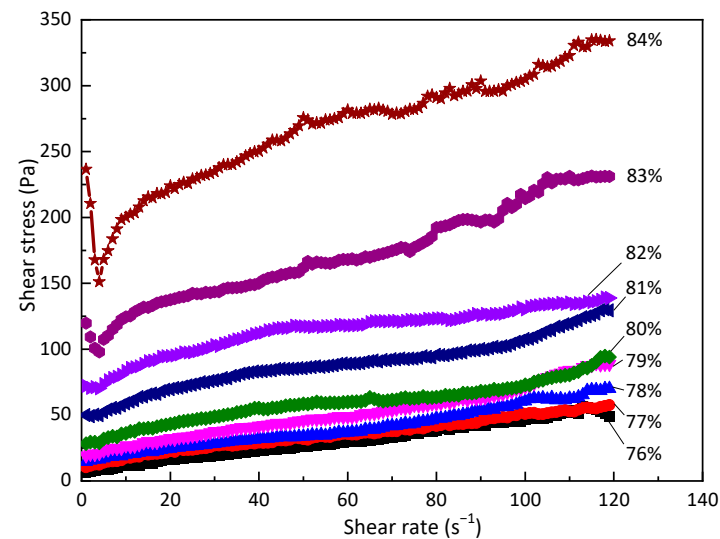


Figure 3. Flow curves of slurry with different concentrations.

Table 1. Rheological parameters based on the flow curve fitting by Bingham model.

	76%	77%	78%	79%	80%	81%	82%	83%	84%
Yield stress (Pa)	7.16	14.84	15.49	22.04	35.25	56.69	79.96	114.85	197.82
Bingham plastic viscosity (Pa·s)	0.39	0.35	0.40	0.46	0.38	0.54	0.64	0.89	1.17

2.2. Experimental Setup

Two L-shaped pipeline systems with internal diameters (ID) of 40 mm and 65 mm, which includes vertical and horizontal sections, were utilized in this study. These two systems had the same composition except for the ID. In this paper, S1 was used to refer to the pipeline system with the ID of 40 mm and S2 is for the ID of 65 mm. Figure 4 provides a schematic drawing of the L-shaped pipeline system. The vertical section is 2 m long and consists of a storage hopper with a capacity of approximately 140 L which is connected to the valve I; several identical pipes with a length of 35 cm are connected with each other by threaded joints; an ERT system comprises a dual-plane ERT sensor, a data acquisition system (DAS) and a host computer used for image reconstruction. The horizontal section is 4 m long and includes several identical pipes with a length of 90 cm; the valve II; a measuring tank and scales to monitor the mass flow. The storage hopper is placed in a stainless-steel stand and the horizontal pipeline is braced by several support frames. With the exception of the ERT sensor, the entire L-shaped pipeline is made of plexiglass which allows for direct observation of the slurry flow.

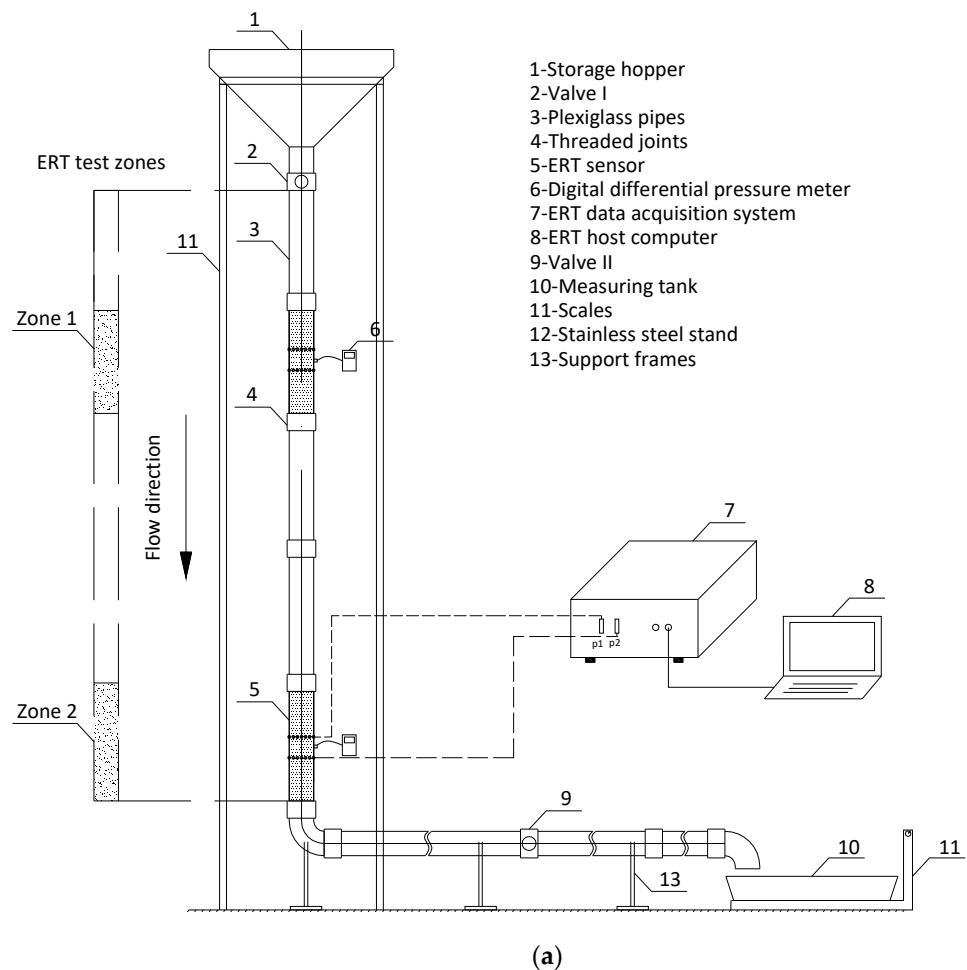
**Figure 4.** Cont.



Figure 4. Gravity flow experimental setup. (a) Schematic drawing; (b) photograph.

The dual-plane ERT sensor is mounted on a uPVC pipe rather than a plexiglass pipe. This is because plexiglass pipes may be more likely to produce cracks in stress concentration areas during the manufacturing process. The distance of two planes is 80 mm, which is used to calculate the slurry axial velocity based on the principle of cross-correlation. Each plane is composed of 16 stainless-steel bolts (DN = 4 mm) acting as electrodes that are mounted on the periphery of the pipe wall at equal intervals. Moreover, each ERT sensor is provided with a port connecting a rubber hose and digital differential pressure-meter used for measuring static pressure. A photograph of ERT sensor with a port is shown in Figure 5. The adjacent electrode pair protocol is employed here which involves injecting the drive current and, subsequently, measuring the voltage difference of adjacent electrodes [44,45]. The ID of the uPVC pipe and each plane being equal to that of plexiglass pipes allows a smooth pipeline inner wall and no interference with the flowing slurry.

Traditional ERT data acquisition systems can acquire up to 200 images per second [26]. A dual-plane V5R system from ITS Ltd., UK, can acquire about 300 frames per second per plane [46]. Gravity transport of backfill in vertical pipes is a rapidly evolving process, where a faster image acquisition speed is required to measure and monitor the flow behavior. Therefore, a high performance ERT system from ITS, which is called Fast Impedance

Camera System (FICA) and can acquire data at a rate of 1000 dual frames per second with an excitation signal frequency of 80 kHz, was used in this research.



Figure 5. Photograph of the ERT sensor.

The gravitational potential energy will accelerate the slurry through the vertical pipe, resulting in a partly filled pipe-flow. A resistance ring was added between the ERT sensor and the DAS in case the slurry falls from the center of the pipe without touching the pipe wall and all electrodes are exposed to the air, which can aid in protecting the ERT systems.

2.3. Experimental Procedure

In order to eliminate noise and reduce error, the ERT system is based on the principle of comparing measured result to a known reference value. It is, thus, necessary to take a reference measurement prior to collecting data. It should be noted that paste slurry can be treated as single-phase flow during the ERT measurement due to its toothpaste-like fluid consistency with no particle segregation. Therefore, the reference frames can be measured when the pipe is full of paste slurry. The experiment includes a set of groups with slurry concentrations of 76%, 78%, 80% and 82%. For each concentration, a reference measurement is required, and pipeline cleaning is essential when any test is completed. About 50 L prepared paste slurry is then poured into the storage hopper. All groups start at the same fluid level and are complete when the slurry is no longer discharged at the end of horizontal pipeline. Figure 6 shows a simplified flowsheet of the ERT experiment operation procedure. Furthermore, the 2-m long vertical pipeline was divided into two test zones from top to bottom, as illustrated in Figure 4. For a given paste slurry to be detected, an ERT sensor would be consecutively mounted on Zone 1 and Zone 2; that is, every group would be repeated at least two times.

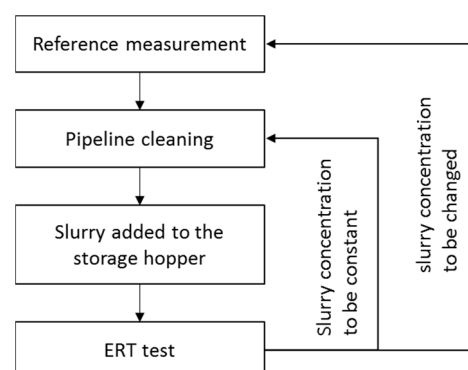


Figure 6. Operation procedure of pipeline transport experiment using ERT.

3. Results and Discussions

3.1. Liquid Holdup

Provided that continuous paste delivery and full-pipe flow are maintained, the risk of pipeline system failures could be largely eliminated. In this paper, liquid holdup (LH), defined as the fraction of a pipe cross-section occupied by slurry, was used to help evaluate the flow patterns of slurry flowing in vertical pipes. Theoretically, a pipeline system with $LH = 0$ means that there is no slurry flowing in the pipe; LH is equal to one when the pipe is completely filled with paste slurry, which is highly beneficial in terms of stability. However, according to the ERT test results, LH ranges from 0.25 to 0.30, the empty pipe is always greater than zero, and the full-pipe flow is less than one due to the resistance ring. LH tested using ERT under different conditions is listed in Table 2.

Table 2. Liquid holdup of paste slurry flowing in the vertical pipe.

	S1-Zone 1	S2-Zone 1	S1-Zone 2	S2-Zone 2
76%	0.75	0.50	0.31	0.32
78%	0.39	0.36	0.93	0.99
80%	0.34	0.26	0.94	0.93
82%	0.33	0.94	0.33	0.94

3.2. Flow Regimes

A large number of two-dimensional concentration tomograms can be obtained from two ERT planes. Images at the same sample interval, collected from a certain plane, can be stacked together by time-series to display a three-dimensional flow pattern, as shown in Figure 7. Each tomogram can be divided into 20×20 square grids. The x-axis and y-axis represent grid nodes (x & $y = 0, 1, 2, \dots, 19, 20$), while the z-axis represents time. In this paper, 50 concentration tomograms under steady-state in which the flow regime is independent of time were stacked to form 3D images. Figure 8 presents flow patterns for paste slurry with mass concentrations of 76%, 78%, 80% and 82% flowing in different zones of S1 and S2. These flow regimes were composed of a series of cross-sections which are the intersection of these 3D images with two planes $x = 10$ and $y = 10$. The area with low conductivity (e.g., air) is shown in blue and the highly conductive material (e.g., slurry) is displayed in red. It is noted that some cases having obvious changes in flow patterns contained two parts which are divided by an arrow. The flow pattern before the arrow depicts an unsteady state and the one after the arrow represents a steady or major state during the test.

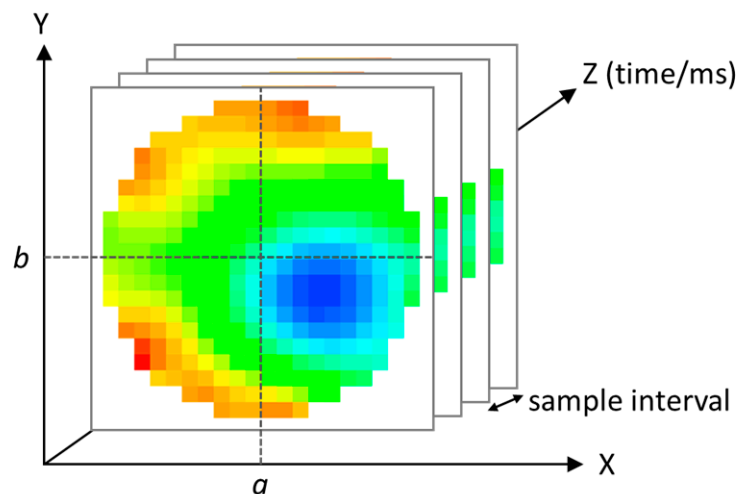
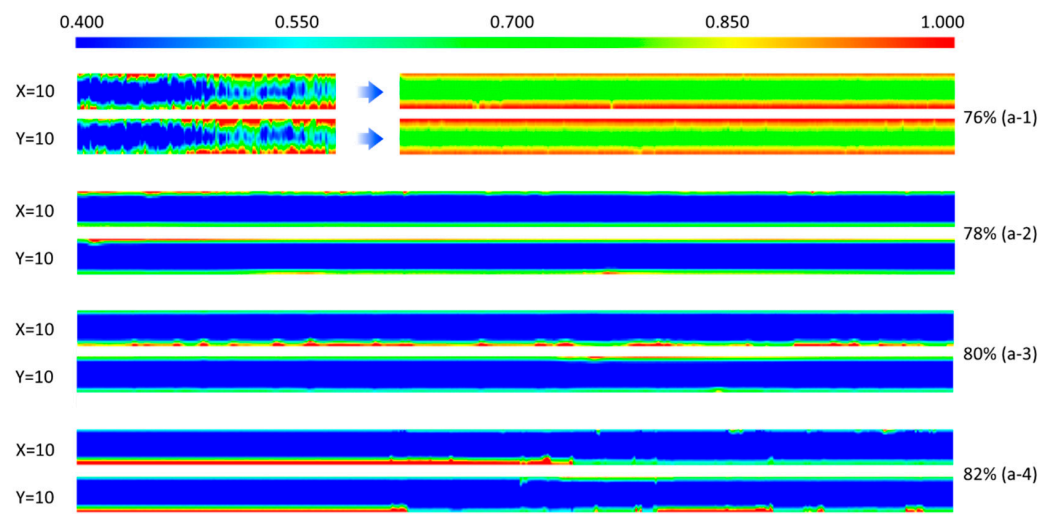
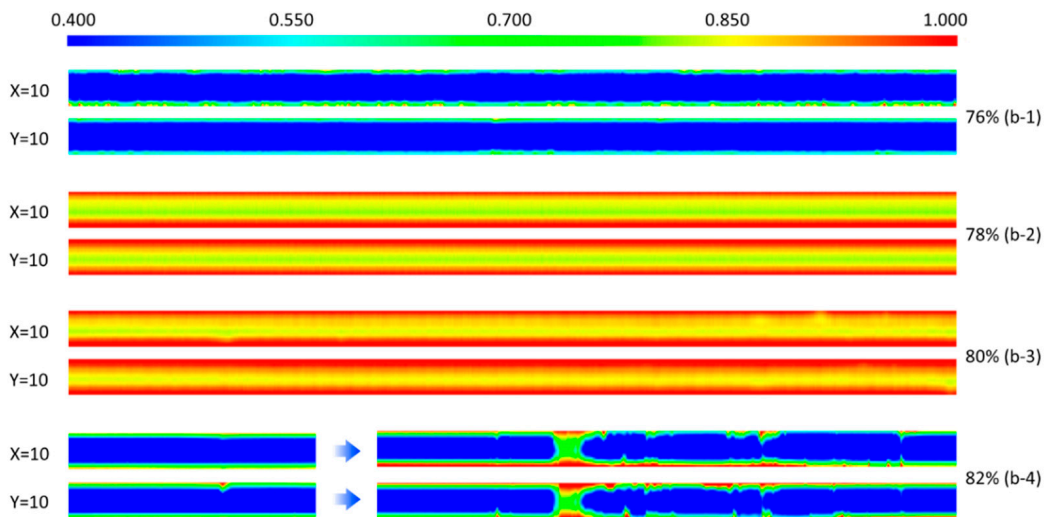


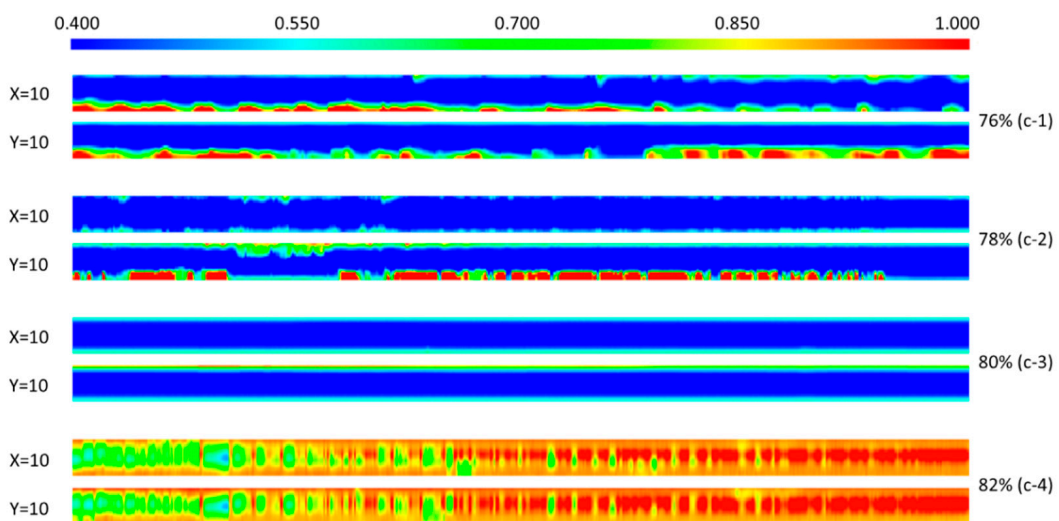
Figure 7. ERT concentration tomograms stacked by time-series.



(a)



(b)



(c)

Figure 8. Cont.

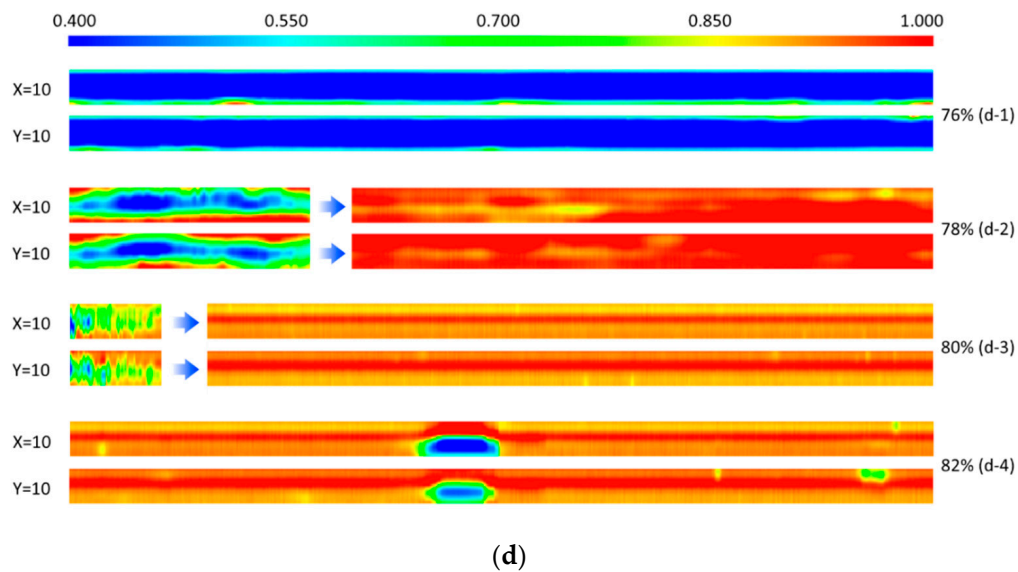


Figure 8. Flow patterns from ERT for paste slurry flowing in vertical pipes. (a) S1-Zone 1; (b) S1-Zone 2; (c) S2-Zone 1; and (d) S2-Zone 2.

3.2.1. Flow Regimes of Slurry Flowing in S1

Figure 8(a-1) shows that a large amount of 76% slurry was poured into the pipe as soon as valve I was opened. The volume of slurry and air in Zone 1 reached the same order of magnitude in a very short time, where local air was pulled into a network by the slurry flow. Some of the air in the vertical pipe was pushed into the storage hopper where the slurry bubbled from time to time, and some was pushed to the downstream position or even the horizontal pipe. Most air bubbles gradually disintegrated as time advanced. One to two seconds after opening the valve I, flow regimes tended to be stable where the liquid holdup of a certain cross-section was about 75%, which indicates the slurry was always trapped with a small amount of air in Zone 1. Figure 8(b-1) illustrates that a very thin slurry layer covered the pipe wall in Zone 2, which prevented researchers from observing what happened inside the pipe. It can be inferred that the slurry was divided by air and only a thin slurry layer on the wall could be detected using ERT, where the LH was 0.31.

The 78% and 80% slurries had similar flow patterns. In Zone 1, only a thin slurry layer flowed along the pipe wall. In this case, the LH had a small value of 0.26 to 0.39, which indicates the pipe was nearly empty. This is clearly unreasonable. In fact, slurry from the storage hopper was divided into two parts, which was occasionally observed from the plexiglass pipes during the test. Besides one part flowing along the pipe wall, another part with a columnar appearance did not contact the pipe wall and was in free fall conditions. As can be seen from Figure 8(b-2,b-3), Zone 2 was completely filled with paste slurry. The flow velocity of the slurry in Zone 2 significantly decreased due to the pipeline resistance at the pipe elbow increasing with the slurry concentration. More low-speed slurry built up near the bottom of the vertical pipe. Thus, the full-pipe flow state was easy to achieve in Zone 2.

LHs of 82% slurry flowing in Zone 1 and Zone 2 were both equal to 0.33. However, the actual flow regime was totally different from 78% or 80% slurry. Partial plugging occurred near valve I due to the paste slurry having high yield stress and viscosity. Only a small amount of broken clumpy slurry fell and very little slurry stuck to the pipe wall. ERT picked up an intermittent signal of slurry dropping down. This explains why the pipe wall areas in Figure 8(a-4) and local small areas in Figure 8(b-4) displayed high conductivity color.

3.2.2. Flow Regimes of Slurry Flowing in S2

The 76% slurry in Zone 1 flowed along the wall pipe and small waves appeared in the air-slurry interface, as illustrated in Figure 8(c-1). Similar to 76% slurry flowing in S1, only a thin slurry layer on the pipe wall of Zone 2 was detected using ERT. Figure 8(d-1) also

shows that the slurry layer thickness in Zone 2 was much thinner than Zone 1, which could be explained by the decrease in the LH from 0.50 in Zone 1 to 0.32 in Zone 2. In this case, it cannot be ignored that some slurry located in the pipe center did not touch the electrodes on the wall.

The interface of air and 78% slurry in Zone 1 tended to be flat, and the LH here was 0.36. The slurry decelerated and accumulated at the bottom of the vertical pipe. The slurry level that was struck by the falling high-speed slurry gradually rose and then remained unchanged where a large number of air bubbles was produced. The LH of 0.99 means that Zone 2 was finally at a state of full-pipe flow, as can be seen from Figure 8(d-2).

For the solid content of 80%, the vertical pipe seemed to be totally empty, as shown in Figure 8(c-3). However, the actual phenomenon during the test was quite different. All of the slurry that fell in a column was located in the center of the pipe, which resulted in there being no flow information obtained using ERT. Figure 8(d-3) shows that Zone 2 was full of slurry and that the final slurry level was higher than in the 78% case.

For the slurry concentration of 82%, the LHs of slurry flowing in Zone 1 and Zone 2 both reached 0.94. The entire vertical pipe was under a full-pipe flow state immediately the 82% slurry was released from the storage hopper. In fact, pipe blockages occurred in the test owing to the excessive pipeline resistance caused by the 82% paste with very high viscosity. Nevertheless, there was still a small number of large bubbles in the slurry, as shown in Figure 8(d-4).

3.2.3. Typical Flow Regimes of Paste Slurry Flowing in Vertical Pipes

According to the above discussion, four types of flow regimes, including mixed flow, columnar flow, stratified flow and full-pipe flow, are defined here and are summarized in Figure 9. These flow regimes are solely defined from the ERT test results for which the classification principle is different from traditional gas-liquid two-phase flow.

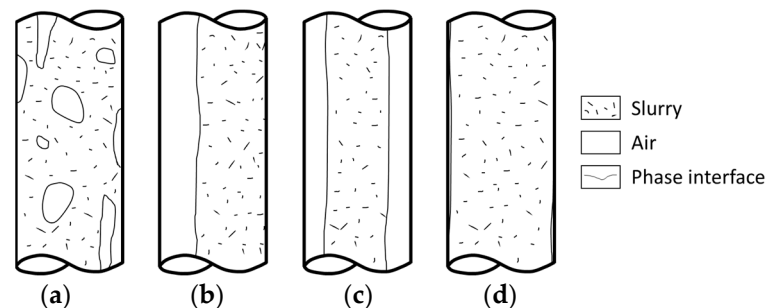


Figure 9. Main flow patterns of paste slurry flowing in vertical pipes. (a) Mixed flow; (b) stratified flow; (c) columnar flow; and (d) full-pipe flow.

Mixed flows can be seen in Figure 8(a-1,d-2,d-3), which is more likely to appear under the following two cases. Case 1 occurs in Zone 1 at the moment that valve I is opened, especially for the lower concentration. The flow regime is significantly affected by boundary mutation. Case 2 happens at the slurry level or phase interface where the flow regimes are changing. During this process, slurry and air are mixed with each other and air bubbles are constantly formed and destroyed, as shown in Figure 9a. Mixed flow is not stable and will eventually be transformed into a steady state.

In the stratified flow, air and slurry are separated from each other and collect on two sides of the pipe wall. Thus, stratified flow has an obvious phase interface. Figure 9b shows that paste slurry flows down along the pipe wall, forming a continuous slurry layer close to the wall surface. As a main flow regime, the stratified flow can occur in most cases. The slurry layer thickness generally become thinner as the slurry falls. In addition, the wetted perimeter, which is the perimeter of the cross-sectional area in contact with the slurry, decreases with the increase in slurry concentration due to the change in the rheological parameter of the paste slurry.

As the name implies, columnar flow has an appearance and shape of a column, as shown in Figure 9c. The falling slurry column, with a path line almost parallel to the pipe axis, finally tapered off to a hanging-drop as the slurry accelerated. The finer slurry column is readily affected by the surrounding air-flow field and then shifts to one side, resulting in contact with the wall of the lower vertical pipe. Columnar flow often appeared together with stratified flow in this experiment. During this experiment, the vertical pipe was directly connected to the storage hopper. Therefore, the slurry in the storage hopper moved vertically downward as soon as valve I was opened, which may be an important factor which led to the columnar flow. However, this is not the case in the majority of currently operational projects. Slurry with a certain velocity flows in the horizontal pipes before reaching the vertical pipes and, subsequently, hits the vertical pipe wall away from the inlet, which is where the flow regime becomes stratified flow.

As illustrated in Figure 8(b-2,b-3,d-2,d-3), full-pipe flow generally occurs in the position near the elbow that connects the vertical pipe and the horizontal pipe due to the reasons discussed in the above section.

3.3. Axial Velocity

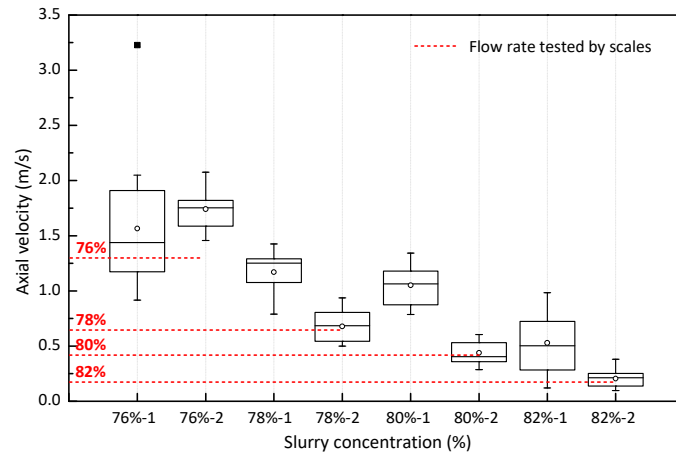
Table 3 lists mass flow rate and mean axial velocity values of slurry flowing in the entire pipeline system measured by the scales at the end of the horizontal pipe. Figure 10 shows boxplots of axial velocity of slurry flowing in Zone 1 and Zone 2 measured using dual-plane ERT. The number '1' or '2' of the x-co-ordinates in Figure 10 represents Zone 1 or Zone 2.

Figure 10 shows that the influence of pipe diameter on the slurry velocity has no obvious logic due to the limited data and small difference between S1 and S2. Nevertheless, some other facts can be also discussed here. The velocity of Zone 1 is less than that of Zone 2 when the slurry concentration is 76%, which indicates that the slurry accelerates between Zone 1 and Zone 2. In this case, Zone 1 and Zone 2 are both in the state of partly-filled pipe-flow, as shown in Figure 8. However, the velocity of Zone 1 is more than that of Zone 2 when the slurry concentration is 78% and 80% (the 82% concentration is not discussed here due to a pipe blockage). The velocity of Zone 2 is basically equal to the mean flow velocities tested using the scales. Figure 8 shows that Zone 1 is in a state of partly-filled pipe-flow and Zone 2 is under a full-pipe flow state. Therefore, the slurry flow velocity is closely related to flow regime transitions. Moreover, the flow velocity fluctuated sharply and there were outliers in Zone 1 when the slurry concentration was 76%. The box body of Zone 2 is generally flatter and shorter than that of Zone 1, which indicates that the flow velocity data of Zone 2 is more concentrated.

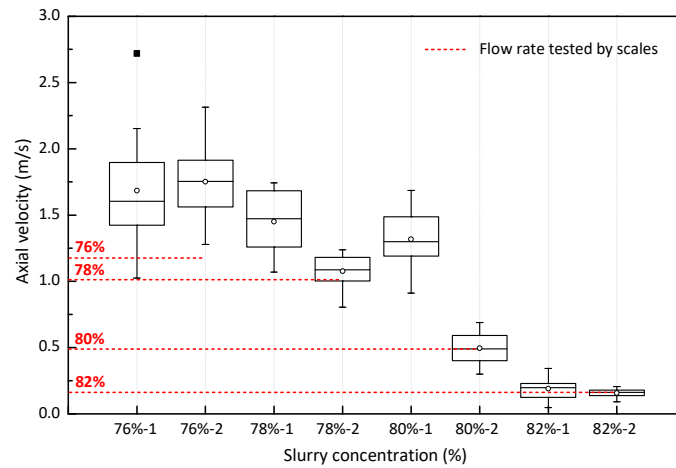
A conclusion to be drawn from the above discussion is that the slurry first accelerates and then remains constant with the increase in the vertical pipe depth. When full-pipe flow occurs near the bottom of the pipe, the velocity suddenly drops at the interface of partly-filled pipe flow and full-pipe flow. Figure 11 shows the process of slurry velocity changing with pipe depth, even though the curve is qualitative and idealized. This process can also be described as partly-filled pipe flow with high-speed which impacts the full-pipe flow with low-speed. Therefore, the interface is not stable because the slurry and air are mixed with each other, air bubbles are constantly formed and destroyed and water-hammer may even occur. Consequently, pipe wear becomes more serious.

Table 3. Flow rate measured by scales.

	S1		S2	
	Mass Flow Rate ($\text{kg}\cdot\text{s}^{-1}$)	Mean Axial Velocity ($\text{m}\cdot\text{s}^{-1}$)	Mass Flow Rate ($\text{kg}\cdot\text{s}^{-1}$)	Mean Axial Velocity ($\text{m}\cdot\text{s}^{-1}$)
76%	3.17	1.30	7.52	1.17
78%	1.57	0.63	6.83	1.03
80%	1.05	0.41	3.33	0.49
82%	0.47	0.18	1.13	0.16



(a)



(b)

Figure 10. Boxplots of axial velocity tested using ERT. (a) S1 and (b) S2.

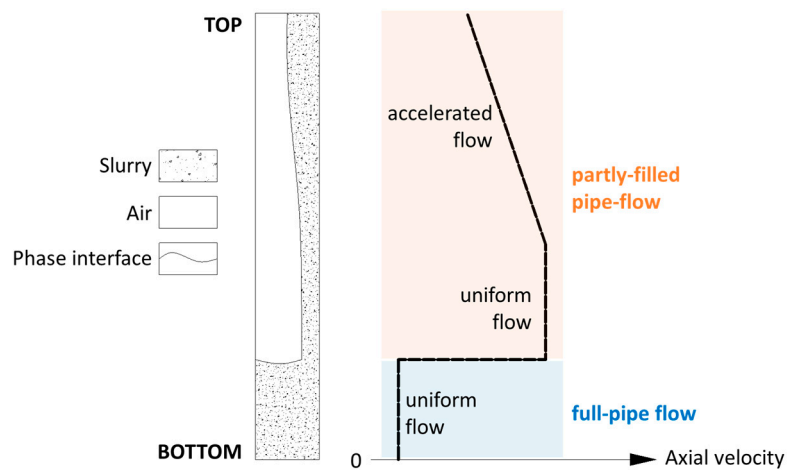
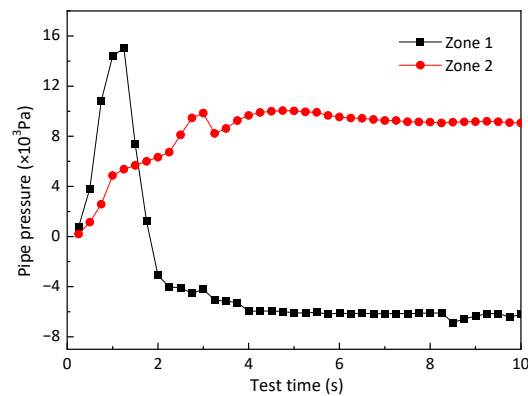


Figure 11. Idealized curve of slurry axial velocity with vertical pipe depth.

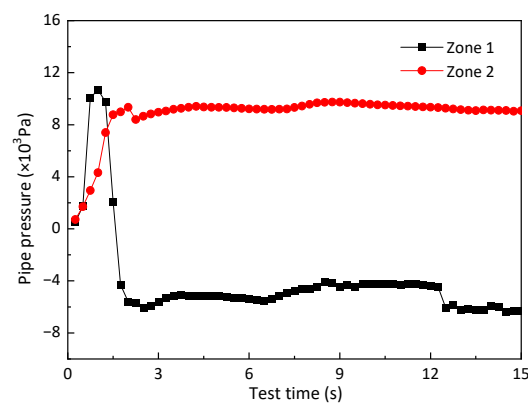
3.4. Pipe Pressure

As soon as valve I is opened, The slurry goes into the pipe and the air in the vertical pipe is rapidly squeezed, and some slurry particles are pushed into the rubber hose, which greatly affects the pressure test results. During this experiment, only three groups, S1-78%,

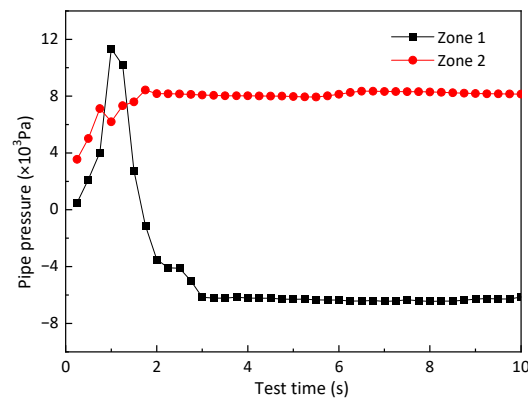
S1-80% and S2-80%, had complete pressure values. Figure 12 shows curves of pressure under different cases changing with test time. The pressure variation trend of these three groups is similar. At the beginning of the test (refer to the first 1 s), the slurry immediately poured into and compressed the air in the pipe, resulting in a sudden increase in the pressure of Zone 1 and Zone 2. The peak pressure of Zone 1 was significantly higher than that of Zone 2. After 1 s, Zone 1 gradually decreased to a negative value, and Zone 2 remained higher than atmospheric pressure and finally tended to be stable. Specifically, in the presence of S1-78%, S1-80% and S2-80%, the stable pressure of Zone 1 was about -6.5 kPa, -5.8 kPa and -6.2 kPa, respectively, and Zone 2 was about 9.6 kPa, 9.5 kPa and 8.2 kPa, respectively.



(a)



(b)



(c)

Figure 12. Pipe pressure with test time in the presence of (a) S1-78%; (b) S1-80% and (c) S2-80%.

During the experiment, the storage hopper was filled with slurry and no air was replenished from the top of the vertical pipe. The partly-filled pipe flow with a certain speed carries the air in Zone 1 downward, resulting in negative pressure in Zone 1, as shown in Figure 13a. In practical projects, the slurry that flows in horizontal pipes has a horizontal velocity and would hit the vertical pipe wall away from the inlet where the flow regime would become stratified flow. In this case, slurry will cover more than half of the vertical pipe section. This phenomenon is called water-tongue, as shown in Figure 13b. Although there are two narrow air channels on each side of the tongue that are not covered by the slurry, the area of air channels is much smaller than the pipe cross-sectional area. The air in the pipe is, thus, divided into two independent parts by the tongue. For the reasons stated, the upper part of the vertical pipe is under negative pressure, which may lead to cavitation erosion.

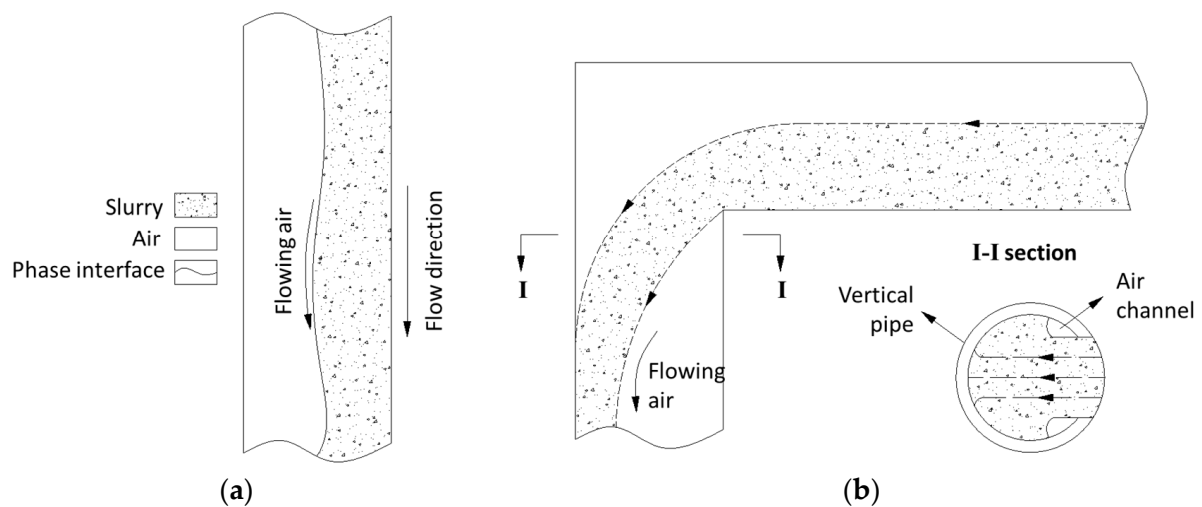


Figure 13. Partly-filled pipe-flow in Zone 1 in the case of (a) experimental pipeline system and (b) practical pipeline system.

4. Future Prospects

Despite the significant experimental studies on paste slurry flowing in vertical pipes, some results limited by the above laboratory conditions might not have extensive adaptability. Firstly, it is essential to improve the experimental setup to get closer to real pipeline systems. Digital differential pressure meters should be replaced with pressure transmitters due to the problems that occurred in current experiment. Secondly, in terms of large-scale or complex conditions, computational fluid dynamics (CFD) numerical simulation could be carried out. Images from the ERT measurement in this paper may be combined with the CFD predictions, which will help to develop a better understanding of slurry flow behavior in vertical pipes. Thirdly, more industrial experiments with larger scale setup are required, where results would be of great reference value and offer practical guidance.

5. Conclusions

Two L-shaped pipeline systems with internal diameters of 40 mm and 65 mm were manufactured to investigate the flow behavior of paste slurry flowing in vertical pipes in which a high performance ERT system was applied. Based on the experimental results, the following conclusions were drawn.

- (1) Four flow regimes, including mixed flow, stratified flow, columnar flow and full-pipe flow, are summarized based on reconstructed images from ERT. These flow regimes are very much affected by the slurry concentration.
- (2) When the slurry concentration was more than 78% in this experiment, full-pipe flow generally occurred in the position near the elbow that connects the vertical pipe and the horizontal pipe.

- (3) For the partly-filled pipe flow, the slurry first accelerates and then remains constant with the increase in the vertical pipe depth. The interface of partly-filled pipe flow and full-pipe flow is not stable, and water-hammer may occur due to the significant speed difference.
- (4) In the presence of S1-78%, S1-80% and S2-80%, the stable pressure of Zone 1 was -6.5 kPa, -5.8 kPa and -6.2 kPa, respectively. Namely, the upper part of the vertical pipe is generally under negative pressure which may lead to cavitation erosion.

Author Contributions: Conceptualization, J.W. and Z.R.; methodology, J.W.; software, Z.R.; validation, J.W., Z.R. and M.W.; formal analysis, J.W. and M.W.; investigation, J.W.; resources, A.W.; data curation, M.W.; writing—original draft preparation, J.W. and Z.R.; writing—review and editing, A.W., M.W. and Z.R.; visualization, J.W. and M.W.; supervision, A.W.; project administration, A.W.; funding acquisition, A.W. and Z.R. All authors have read and agreed to the published version of the manuscript.

Funding: This research was funded by the National Natural Science Foundation of China (No. 52130404), China Postdoctoral Science Foundation (No. 2021M690011), Guangdong Basic and Applied Basic Research Foundation (No. 2021A1515110161) and Postdoctor Research Foundation of Shunde Graduate School of University of Science and Technology Beijing (No. 2021BH011).

Acknowledgments: The authors would like to acknowledge the great support provided by Hua Li from Institute of Mechanics, Chinese Academy of Sciences and Haibo Jin from Beijing Institute of Petrochemical Technology. We also want to thank Yi Mo, Xiuhan Hu, Guangyi Yu and Longsen Yuan for their help in the experiment.

Conflicts of Interest: The authors declare that they have no known competing financial interest or personal relationships that could have appeared to influence the work reported in this paper.

References

1. Zhang, Y.; Liu, B.; Gu, X.; Nehdi, M.L.; Zhang, L.V. Mechanochemical activation of iron ore tailing-based ternary supplementary cementitious materials. *Constr. Build. Mater.* **2022**, *346*, 128420. [[CrossRef](#)]
2. Wang, X.; Wang, H.; Wu, A.; Kang, G. Wear law of Q345 steel under the abrasion–corrosion synergistic effect of cemented paste backfill. *Constr. Build. Mater.* **2022**, *332*, 127283. [[CrossRef](#)]
3. Wu, A.; Ruan, Z.; Wang, J. Rheological behavior of paste in metal mines. *Int. J. Miner. Metall. Mater.* **2022**, *29*, 717–726. [[CrossRef](#)]
4. Abdul-Hussain, N.; Fall, M. Thermo-hydro-mechanical behaviour of sodium silicate-cemented paste tailings in column experiments. *Tunn. Undergr. Space Technol.* **2012**, *29*, 85–93. [[CrossRef](#)]
5. Yan, Z.; Yin, S.; Chen, X.; Wang, L. Rheological properties and wall-slip behavior of cemented tailing-waste rock backfill (CTWB) paste. *Constr. Build. Mater.* **2022**, *324*, 126723. [[CrossRef](#)]
6. Qi, C.; Fourie, A. Cemented paste backfill for mineral tailings management: Review and future perspectives. *Miner. Eng.* **2019**, *144*, 106025. [[CrossRef](#)]
7. Jiang, H.; Fall, M.; Yilmaz, E.; Li, Y.; Yang, L. Effect of mineral admixtures on flow properties of fresh cemented paste backfill: Assessment of time dependency and thixotropy. *Powder Technol.* **2020**, *372*, 258–266. [[CrossRef](#)]
8. Fall, M.; Adrien, D.; Célestin, J.C.; Pokharel, M.; Touré, M. Saturated hydraulic conductivity of cemented paste backfill. *Miner. Eng.* **2009**, *22*, 1307–1317. [[CrossRef](#)]
9. Jewell, R.J.; Fourie, A.B. *Paste and Thickened Tailings: A Guide*; Australian Centre for Geomechanics, The University of Western Australia: Perth, Australia, 2006.
10. Ranjith, P.G.; Zhao, J.; Ju, M.; de Silva, R.V.S.; Rathnaweera, T.D.; Bandara, A.K.M.S. Opportunities and Challenges in Deep Mining: A Brief Review. *Engineering* **2017**, *3*, 546–551. [[CrossRef](#)]
11. Emad, M.Z.; Mitri, H.; Kelly, C. State-of-the-art review of backfill practices for sublevel stoping system. *Int. J. Min. Reclam. Environ.* **2014**, *29*, 544–556. [[CrossRef](#)]
12. Sinha, S.L.; Dewangan, S.K.; Sharma, A. A review on particulate slurry erosive wear of industrial materials: In context with pipeline transportation of mineral–slurry. *Part. Sci. Technol.* **2015**, *35*, 103–118. [[CrossRef](#)]
13. Popescu, D.P.; Choo-Smith, L.P.; Flueraru, C.; Mao, Y.; Chang, S.; Disano, J.; Sherif, S.; Sowa, M.G. Optical coherence tomography: Fundamental principles, instrumental designs and biomedical applications. *Biophys. Rev.* **2011**, *3*, 155. [[CrossRef](#)]
14. Iijima, M.; Taki, N.; Tatami, J. Operando observation of concentrated SiO₂ suspensions by optical coherent tomography during flow curve measurements: The relationship between polymer dispersant structures and surface interactions. *J. Colloid Interface Sci.* **2022**, *607*, 290–297. [[CrossRef](#)]
15. Abbagoni, B.M.; Yeung, H.; Lao, L. Non-invasive measurement of oil-water two-phase flow in vertical pipe using ultrasonic Doppler sensor and gamma ray densitometer. *Chem. Eng. Sci.* **2022**, *248*, 117218. [[CrossRef](#)]

16. Salgado, C.M.; Dam, R.S.d.F.; Conti, C.d.C.; Salgado, W.L. Three-phase flow meters based on X-rays and artificial neural network to measure the flow compositions. *Flow Meas. Instrum.* **2021**, *82*, 102075. [[CrossRef](#)]
17. Li, T.-Q.; McCarthy, K.L. Pipe flow of aqueous polyacrylamide solutions studied by means of nuclear magnetic resonance imaging. *J. Non-Newtonian Fluid Mech.* **1995**, *57*, 155–175. [[CrossRef](#)]
18. Lev, E.; Boyce, C.M. Opportunities for Characterizing Geological Flows Using Magnetic Resonance Imaging. *iScience* **2020**, *23*, 101534. [[CrossRef](#)]
19. Thorn, R.; Johansen, G.A.; Hammer, E.A. Recent developments in three-phase flow measurement. *Meas. Sci. Technol.* **1997**, *8*, 691–701. [[CrossRef](#)]
20. Faraj, Y.; Wang, M. ERT Investigation on Horizontal and Vertical Counter-gravity Slurry Flow in Pipelines. *Procedia Eng.* **2012**, *42*, 588–606. [[CrossRef](#)]
21. Qureshi, M.F.; Ali, M.H.; Ferroudji, H.; Rasul, G.; Khan, M.S.; Rahman, M.A.; Hasan, R.; Hassan, I. Measuring solid cuttings transport in Newtonian fluid across horizontal annulus using electrical resistance tomography (ERT). *Flow Meas. Instrum.* **2021**, *77*, 101841. [[CrossRef](#)]
22. Rodgers, T.; Kowalski, A. An electrical resistance tomography method for determining mixing in batch addition with a level change. *Chem. Eng. Res. Des.* **2010**, *88*, 204–212. [[CrossRef](#)]
23. Sharifi, M.; Young, B. Electrical resistance tomography (ERT) for flow and velocity profile measurement of a single phase liquid in a horizontal pipe. *Chem. Eng. Res. Des.* **2013**, *91*, 1235–1244. [[CrossRef](#)]
24. Sharifi, M.; Young, B. 3-Dimensional spatial monitoring of tanks for the milk processing industry using electrical resistance tomography. *J. Food Eng.* **2011**, *105*, 312–319. [[CrossRef](#)]
25. Sharifi, M.; Young, B. Electrical Resistance Tomography (ERT) applications to Chemical Engineering. *Chem. Eng. Res. Des.* **2013**, *91*, 1625–1645. [[CrossRef](#)]
26. Dyakowski, T.; Jeanmeure, L.F.C.; Jaworski, A.J. Applications of electrical tomography for gas–solids and liquid–solids flows—A review. *Powder Technol.* **2000**, *112*, 174–192. [[CrossRef](#)]
27. Polansky, J.; Wang, M. Vertical annular flow pattern characterisation using proper orthogonal decomposition of Electrical Impedance Tomography. *Flow Meas. Instrum.* **2018**, *62*, 281–296. [[CrossRef](#)]
28. Tan, C.; Zhao, J.; Dong, F. Gas-water two-phase flow characterization with Electrical Resistance Tomography and Multivariate Multiscale Entropy analysis. *ISA Trans.* **2015**, *55*, 241–249. [[CrossRef](#)]
29. Dong, F.; Xu, Y.; Xu, L.; Hua, L.; Qiao, X. Application of dual-plane ERT system and cross-correlation technique to measure gas–liquid flows in vertical upward pipe. *Flow Meas. Instrum.* **2005**, *16*, 191–197. [[CrossRef](#)]
30. Giguère, R.; Fradette, L.; Mignon, D.; Tanguy, P. Characterization of slurry flow regime transitions by ERT. *Chem. Eng. Res. Des.* **2008**, *86*, 989–996. [[CrossRef](#)]
31. Hashemi, S.; Sadighian, A.; Shah, S.; Sanders, R. Solid velocity and concentration fluctuations in highly concentrated liquid–solid (slurry) pipe flows. *Int. J. Multiph. Flow* **2014**, *66*, 46–61. [[CrossRef](#)]
32. Mahmud, M.; Faraj, Y.; Wang, M. Visualisation and Metering of Two Phase Counter-gravity Slurry Flow using ERT. *Procedia Eng.* **2015**, *102*, 930–935. [[CrossRef](#)]
33. Gharib, N.; Bharathan, B.; Amiri, L.; McGuinness, M.; Hassani, F.P.; Sasmito, A.P. Flow characteristics and wear prediction of Herschel-Bulkley non-Newtonian paste backfill in pipe elbows. *Can. J. Chem. Eng.* **2017**, *95*, 1181–1191. [[CrossRef](#)]
34. Matoušek, V.; Krupička, J. One-dimensional modeling of concentration distribution in pipe flow of combined-load slurry. *Powder Technol.* **2014**, *260*, 42–51. [[CrossRef](#)]
35. Machin, T.D.; Wei, H.; Greenwood, R.W.; Simmons, M.J.H. In-pipe rheology and mixing characterisation using electrical resistance sensing. *Chem. Eng. Sci.* **2018**, *187*, 327–341. [[CrossRef](#)]
36. Feng, G.; Wang, Z.; Qi, T.; Du, X.; Guo, J.; Wang, H.; Shi, X.; Wen, X. Effect of velocity on flow properties and electrical resistivity of cemented coal gangue-fly ash backfill (CGFB) slurry in the pipeline. *Powder Technol.* **2022**, *396*, 191–209. [[CrossRef](#)]
37. Liu, L.; Fang, Z.; Wu, Y.; Lai, X.; Wang, P.; Song, K. Experimental investigation of solid-liquid two-phase flow in cemented rock-tailings backfill using electrical resistance tomography. *Constr. Build. Mater.* **2018**, *175*, 267–276. [[CrossRef](#)]
38. Wu, D.; Yang, B.; Liu, Y. Pressure drop in loop pipe flow of fresh cemented coal gangue–fly ash slurry: Experiment and simulation. *Adv. Powder Technol.* **2015**, *26*, 920–927. [[CrossRef](#)]
39. Doron, P.; Barnea, D. Pressure drop and limit deposit velocity for solid-liquid flow in pipes. *Chem. Eng. Sci.* **1995**, *50*, 1595–1604. [[CrossRef](#)]
40. Fu, W.; Yu, J.; Xiao, Y.; Wang, C.; Huang, B.; Sun, B. A pressure drop prediction model for hydrate slurry based on energy dissipation under turbulent flow condition. *Fuel* **2022**, *311*, 122188. [[CrossRef](#)]
41. Zhang, Q.; Cui, J.; Zheng, J.; Wang, X.; Wang, X. Wear mechanism and serious wear position of casing pipe in vertical backfill drill-hole. *Trans. Nonferrous Met. Soc. China* **2011**, *21*, 2503–2507. [[CrossRef](#)]
42. Xiao, B.; Wen, Z.; Wu, F.; Li, L.; Yang, Z.; Gao, Q. A simple L-shape pipe flow test for practical rheological properties of backfill slurry: A case study. *Powder Technol.* **2019**, *356*, 1008–1015. [[CrossRef](#)]
43. Zhang, Q.-L.; Hu, G.-Y.; Wang, X.-M. Hydraulic calculation of gravity transportation pipeline system for backfill slurry. *J. Central South Univ. Technol.* **2008**, *15*, 645–649. [[CrossRef](#)]
44. Dickin, F.; Wang, M. Electrical resistance tomography for process applications. *Meas. Sci. Technol.* **1996**, *7*, 247–260. [[CrossRef](#)]

-
45. Brown, B.H.; Barber, D.C.; Seagar, A.D. Applied potential tomography: Possible clinical applications. *Clin. Phys. Physiol. Meas.* **1985**, *6*, 109–121. [[CrossRef](#)] [[PubMed](#)]
 46. Hashemi, S.; Spelay, R.; Sanders, R.; Hjertaker, B. A novel method to improve Electrical Resistance Tomography measurements on slurries containing clays. *Flow Meas. Instrum.* **2021**, *80*, 101973. [[CrossRef](#)]